Finite-State Induced-Flow Model for Rotors in Hover and Forward Flight

David A. Peters
Professor

David Doug Boyd
Research Assistant

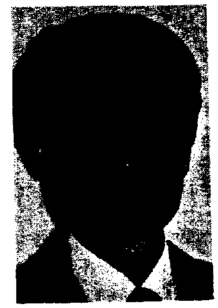

Cheng Jian He
Research Assistant

School of Aerospace Engineering
Georgia Institute of Technology
Atlanta, Ga.

A theory of unsteady aerodynamics (in terms of induced flow) is offered for a lifting rotor in hover and forward flight. The induced flow is expressed azimuthally by a Fourier series and radially by Legendre functions. The magnitude of each term is determined from first-order differential equations in either the time or frequency domain. The coefficients of the differential equations depend only on the wake skew angle. The forcing functions are user-supplied, radial integrals of the blade loadings. In a nonlifting climb, the theory gives results almost identical to those of Loewy theory but with improved values of the wake apparent mass and correct tip-loss behavior. The theory implicitly includes dynamic-inflow theory, the Prandtl/Goldstein static inflow distribution, and Theodorsen theory. Finally, comparisons with other theories and experimental data show the theory to be accurate even up to 1,000 harmonics.

Notation

a	= slope of lift curve, 1/rad
$A, A(k)$	= induced-flow factor
$[\underline{A}^m], [\underline{B}^m]$	= matrices of integrals
$[\bar{A}^m], [\bar{B}^m]$	= special case of $[A^m]$ and $[B^m]$
b	= blade semi-chord, $c/2$, m
$\hat{b}, \bar{b}$	= dimensionless semi-chord, $\hat{b}/x$, b/R
B	= tip-loss factor
c	= blade chord, m
$\bar{c}$	= dimensionless blade chord, c/R
$\delta C_L, \delta C_M$	= perturbation rolling and pitching moment coefficients
δC_T	= perturbation thrust coefficient
$\bar{C}_T$	= steady thrust coefficient
C_T	= total thrust coefficient, $\bar{C}_T + \delta C_T$
$C[\,]$	= induced flow operator
$C(k)$	= Theodorsen Function
$C'(k)$	= Loewy Function
C_n^m, D_n^m	= coefficients of potential function
f_m	= chordwise distribution function
F', G'	= real and imaginary parts of $C'(k)$
h	= wake spacing divided by semi-chord
j	= blade-passage index, column index
J	= number of blade-passage harmonics
J_0, J_1	= Bessel Functions
k	= reduced freq. in rotating system, $\hat{b}\omega_R$
k_m	= reduced frequency of m-th harmonic, $\hat{b}m$
K_n^m	= apparent-mass diagonals
L_c	= circulatory lift/unit span, N/m
L_{cq}	= nondimensional lift of qth blade $L_c/\rho\Omega^2R^3$
$[L]$	= matrix of inflow gains
$[L^c], [L^s]$	= matrix of harmonic couplings
$L[\,]$	= static inflow operator
M	= total number of harmonics
$[M]$	= apparent mass matrix
m	= harmonic number
n	= polynomial number
$\bar{p}$	= flapping frequency, per/rev
p	= polynomial number
$P_q(r,y,t)$	= pressure distribution of qth blade, pressure/$\rho\Omega^2R^2$
$P_y(y)$	= chordwise pressure function
$P_n^m(\nu)$	= Legendre functions
$\bar{P}_n^m(\nu)$	= normalized functions, $(-1)^m P_n^m(\nu)/\rho_n^m$
q	= blade index
Q	= number of blades
$Q_n^m(i\eta)$	= associated Legendre functions
$\bar{Q}_n^m(i\eta)$	= normalized functions, $Q_n^m(i\eta)/Q_n^m(i0)$
r	= harmonic number
$\bar{r}$	= normalized radial position, x/R
R	= rotor radius, m
s	= cyclic harmonic, Table II

*This paper was presented at the 43rd Annual Forum of the American Helicopter Society, St. Louis, Mo., May 18–20, 1987.

S = number of shape functions per harmonic
t = power of $\bar{r}$ in distribution, Eq. (30) only
t = time, sec
$\bar{t}$ = nondimensional time, $= \Omega t$
T_m = time constant of m-th harmonic at $V=1$
U_I = induced velocity at airfoil m/sec
U_P = velocity normal to airfoil m/sec
U = velocity relative to airfoil m/sec
V = mass-flow parameter
w = induced velocity at rotor disc, velocity/ΩR
W = Loewy wake-spacing function
x = radial coordinate, m
y = chordwise coordinate, positive downstream, divided by R
Y_0, Y_1 = Bessel functions of second kind
z = coordinate normal to rotor, $/R$
α = wake skew angle at disc, rad, zero for axial flow
α_n^m, β_n^m = induced-flow coefficients
β = blade flapping angle, rad
γ = blade Lock number
δ_{ps} = Kronecker delta
η = ellipsoidal coordinate, $= 0$ on disc
θ = blade pitch angle, rad
$\theta_o, \theta_s, \theta_c$ = collective and cyclic pitch, rad
θ_q = pitch angle of q-th blade, rad
λ = free-stream flow normal to disc, divided by ΩR
$\lambda_{mc}, \lambda_{ms}$ = inflow variables, Ref. 23
λ_I = induced flow at blade, $U_I/\Omega R$, in two-dimensional model
λ_I^m = mth harmonic of λ_I in two-dimensional model
Λ^m = weighting function
μ = advance ratio
$\bar{\nu}$ = momentum-theory value of nondimensional, uniform inflow
ν = ellipsoidal coordinate
ν_0 = ν from which ξ originates
ξ = nondimensional coordinate along streamline, positive upstream
ρ = density of air, kg/m
$(\rho_n^m)^2$ = integral (0 to 1) of $(P_n^m)^2$, $\dfrac{1}{2n+1}\dfrac{(n+m)!}{(n-m)!}$
σ = rotor solidity, $Qc/(\pi R)$
τ_n^{mc}, τ_n^{ms} = coefficients of pressure expansion
$\Phi(\nu, \eta, \bar{\psi}, t)$ = acceleration potential, pressure/$\rho\Omega^2R^2$
$\phi(\nu, \bar{\psi}, t)$ = pressure across disc divided by $\rho\Omega^2R^2$
X = wake skew parameter, $\tan(\alpha/2)$
ψ = azimuthal position on rotor disc, rad
ψ_q = spatial position of q-th blade, rad
$\bar{\psi}$ = ellipsoidal coordinate, $= \psi$ on disc
$\psi_s^m(\nu)$ = assumed velocity distributions
ψ_0 = $\bar{\psi}$ from which ξ originates
$\omega \equiv \omega_n$ = per-rev frequency in nonrotating system
$\omega_R \equiv \omega_r$ = per-rev frequency in rotating frequency
Ω = rotor speed, rad/sec
$(m)!!$ = $(m)(m-2)(m-4)\ldots(2 \text{ or } 1)$, $(-3)!! = -1$, $(-1)!! = 1$, $(0)!! = 1$, Refs. 26–27
$(\dot{\ })$ = $d(\ )/dt$
$({}^*)$ = $d(\ )/d\bar{t}$
$(\ )^A$ = due to flow acceleration
$(\ )^V$ = due to momentum flux

Introduction

Classical Unsteady Theories

Although there are a great number of research tools that have increased our understanding of rotor unsteady aerodynamics, there are only a very few unsteady aerodynamic theories that can be applied to realistic problems of helicopter dynamics. Perhaps the most fundamental tool is Theodorsen theory, Ref. 1, which is often included in rotor analyses. The Theodorsen theory for lift contains both circulatory and noncirculatory terms. The circulatory terms take the form of a quasi-steady lift multiplied by a lift-deficiency function, $C(k)$,

$$L_c = 2\pi\rho bU(U_p + b\dot{\Theta}/2)C(k) \tag{1}$$

where U_p is the velocity normal to the blade at mid-chord. To understand the nature of this unsteady aerodynamic behavior, it is interesting to rewrite Eq. (1) in terms of the flow induced by the shed vorticity, U_I.

$$L_c = 2\pi\rho bU(U_p + b\dot{\Theta}/2 - U_I) \tag{2a}$$

$$U_I = A(k)L_c/(2\pi\rho bU) \tag{2b}$$

$$L_c = 2\pi\rho bU(U_p + b\dot{\Theta}/2)\frac{1}{1 + A(k)} \tag{2c}$$

The feedback constant, $A(k)$, relates the induced flow at the midchord to the circulation shed from the blade. It is directly related to $C(k)$ by the relationship

$$C(k) = \frac{1}{1 + A(k)} \tag{3}$$

We find that $A(k)$ in Theodorsen theory is expressed more simply than is $C(k)$.

$$A(k) = \frac{Y_0(k) + iJ_0(k)}{J_1(k) - iY_1(k)} \tag{4}$$

Figure 1 illustrates the relationship between Eq. (2) and a blade dynamics problem. We see that blade aerodynamics can usually be separated into two distinct theories. One theory, the forward loop, relates the flow field at the blade (e.g., angle of attack, gradient, rates, etc.) to the lift and circulation developed on the blade. This implies the use of Eq. (2a), for the circulatory lift, and the use of standard apparent mass terms for the noncirculatory lift. The second theory, the upper feedback loop, relates the time-history of circulatory lift on the blade to the resultant induced flow at the blade, Eqs. (2b) and (4). The blade dynamic theory need not affect these aerodynamic theories. In other words, despite the fact that blade motions enter into the angle of attack, the blade lifting theory can be derived

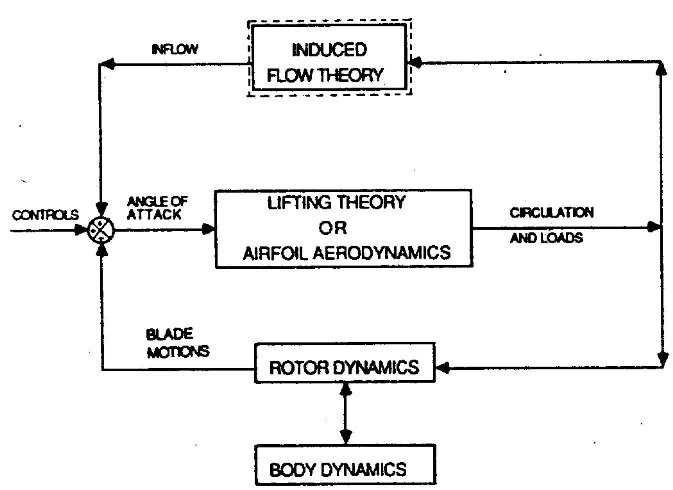

Fig. 1. Block diagram of inflow as open loop (---) and closed loop (————) systems.

independently of the blade dynamic theory (the lower feedback loop in Fig. 1). Similarly, despite the fact that the induced flow enters the angle of attack, the induced-flow theory can be developed independently of the blade-lift theory. In other words, L_c and $A(k)$ can be considered independently.

The validity of this point of view can be further seen in Loewy theory, Ref. 2. There, the same flat-plate airfoil is used as in Theodorsen theory. Thus, there is no change in the relationship between velocity field and circulation; Eq. (2a) remains unchanged. However, Ref. 2 does alter the induced-flow theory by introducing layers of vorticity (spaced apart by h semichords) that simulate the rotor wake. The resultant lift-deficiency function can be expressed as in Eq. (3) with $A(k)$ given by

$$A(k) = \frac{Y_0(k) + iJ_0(k)(1 + 2W)}{J_1(k)(1 + 2W) - iY_1(k)} \tag{5}$$

The Loewy wake-spacing function, W, accounts for the layers of vorticity in a 2-dimensional manner. It is given by

$$W = [\exp(kh + 2\pi i\omega/Q) - 1]^{-1} \tag{6}$$

where ω is the frequency in the nonrotating system. Thus, Loewy theory allows for the separation of lift theory and induced-flow theory, as indicated by Eq. (2).

We should also mention the work of Miller, Ref. 3. His 3-dimensional theory similarly can be divided into lift theory and induced-flow theory, although the latter theory is not obtained in closed form for general k. However, his 2-dimensional theory can be obtained in closed form with

$$A(k) = \frac{Y_0(k) + i(J_0(k) + 2W)}{J_1(k) - iY_1(k)} \tag{7}$$

Equations (5) and (7) give nearly identical results for parameters typical of helicopters. In fact, they have the same near-wake approximation, Ref. 4.

$$A(k) = \pi k/2 + \pi kW = \pi k(1/2 + W) \tag{8}$$

Equation (8) has some interesting properties which will be of interest both here and later in this paper. First, we note that $\pi k/2$ is the near-wake approximation to either Theodorsen theory or Sears theory (lift-deficiency for gust response); and this near-wake theory is valid for $k < 1.0$ (which is realistic for helicopters), Ref. 4. Thus, Eq. (8) is a reasonable approximation of classical, unsteady aerodynamics for a rotor. Second, we note from Eq. (6) that for small wake spacing, $kh < .5$, W oscillates between $-1/2$ and $1/kh$, the latter occurring as sharp spikes at integer multiples of the blade number ($\omega = jQ$). Therefore, $A(k)$ varies between 0 and π/h; and $C'(k)$ varies between 1 and $h/(h + \pi)$. An interesting conclusion is that, away from these sharp spikes (for which $W = -1/2$, $A = 0$), the effect of the two-dimensional rotor wake is to negate the major portion of the Theodorsen function, $\pi k/2$.

Need for Advanced Theories

In the preceding discussion of classical unsteady aerodynamics, we have seen that Theodorsen theory is not only inadequate; but it is probably counter-productive for rotor analyses. A logical conclusion from this might be that we ought to use only Loewy theory. However, there are several aspects of Loewy theory that make it less than ideal for aeroelastic analysis.

First, the theory is for the linear aerodynamics of a flat-plate airfoil, whereas we need a theory that can be combined with more sophisticated airfoil theories. The second drawback of Loewy theory is that it is a two-dimensional theory. Therefore, it does not account for radial coupling of thrust and induced flow. A third problem is that the theory is strictly for a low-lift climb. Although the "low-lift" part can be overcome by use of a modified wake spacing, the "climb" part means that we have no way of applying the theory in forward flight, which is exactly the condition for which we most need unsteady aerodynamics. Fourth, Loewy theory, like all of the classical unsteady theories, is in the frequency domain. This makes it inappropriate for conventional aeroelastic eigenvalue analysis (with the possible exception of V–g plots for stability boundaries in hover). One cannot even iteratively assign a k to each mode due to the facts that: 1) significant damping is present in flap and 2) multiple frequencies occur for each mode in forward flight. Lastly, the Loewy function has a singularity in the collective mode at $\omega = k = 0$ which gives $C'(0)$ a finite imaginary part. (This singularity is usually overlooked in the literature because we often fix either ω or k and let the other go to zero rather than taking the limit as they both go to zero.)

Given these shortcomings of classical theories of unsteady aerodynamics, we might look to more sophisticated theories that could be used in rotor aeroelasticity. The most well-known of such theories would certainly be prescribed-wake lifting-line theories, Refs. 5–6, free-wake lifting-line theories, Ref. 7, and lifting surface theories, Ref. 8. Interestingly, these also can be expressed in the framework of the block diagram of Fig. 1. In particular, the lift part of the theories either relate the circulation of a lifting line to the blade circulation (as computed by some formula), or else they adjust the circulation of panels so as to match a boundary condition at the blade. Such a lift calculation only requires the local flow field as an input. Therefore it qualifies as the forward loop of Fig. 1. The induced-flow calculation (or feedback loop) of these vortex theories is found from the Biot-Savart Law as applied to the geometry of the wake. Thus, different assumptions on wake geometry can change the induced-flow theory without changing the lifting theory. These vortex methods can include a sophisticated wake that is three-dimensional with wake contraction in forward flight. Therefore, the more advanced wake models can overcome all of the deficiencies of Loewy theory. Such methods stand as important tools for helicopter analysis.

However, when we come to the question of performing an aeroelastic analysis of a realistic rotor, we find that vortex-filament theories are not presently a viable alternative. First of all, for any problem beyond rigid-blade flapping, the computational effort of tracking the unsteady vorticity and of computing induced-flow integrals over hundreds of filaments at every time step is simply too large to handle on a routine basis. Second, these vortex theories are restricted to time-marching problems. They are not in a format that would allow eigenvalue analysis. Even Floquet solutions, which entail time-marching over one period, cannot be applied because the states of the flow field either are not defined or involve too many wake degrees of freedom. One can impose restrictions that allow a more closed-form version of vortex theories. Such restrictions include a cylindrical wake and an infinite number of blades, Ref. 4. Several authors have developed such theories, Refs. 3 and 9–12; but the assumption of an infinite number of blades restricts the results to only the first or second harmonic of induced flow.

As a final point on the need for a better induced flow theory, we consider advanced theories for the blade-lift portion of Fig. 1. Many of these are two-dimensional, dynamic-stall theories that rely on classical methods (e.g., convolution with a Wagner function) to obtain the wake, Refs. 13–14. Others are more sophisticated Euler or Navier-Stokes solvers. These solve a finite-difference mesh near the blade but rely on other estimates for the induced flow entering that mesh, Ref. 15. Because these theories can separate the blade theory from the induced-flow theory, and because they presently utilize very primitive wake models, these theories could also benefit from an alternative induced-flow model for rotors.

Finite-State Models

One type of induced-flow formulation that holds promise for aeroelasticity calculations is the class of finite-state models. Such models are formulated as differential equations for the unknown states of the flow field. This type of formulation allows direct computation of Floquet or constant-coefficient eigenvalues while not precluding time-history or frequency-domain analyses. The difficulty, however, is in the extraction of a finite-state model from an adequate aerodynamic theory. For the classical treatment of two-dimensional aerodynamics, researchers have used trial and error to obtain one- and two-pole approximations to the Wagner and Küssner responses, Ref. 16. (Such a treatment is used in Ref. 14 in combination with dynamic stall.)

Friedmann, Refs. 17–18, has applied Bode Plot methods to fit multiple-pole approximations to both Theodorsen and Loewy theories. These involve up to 17 poles (i.e., 17 extra state variables) at each radial position. An alternative method of obtaining a finite-state model is given in Ref. 19. Interestingly, this reference shows that finite-state models also fall into the category of the schematic in Fig. 1. In fact, Ref. 19 refers directly to the "feed-forward" and "feedback" portions of the model. References 17–19 provide an important improvement toward a useful induced-flow model in that they remove the frequency-domain limitation of classical models. However, the other problems with classical theories remain (e.g., no forward-flight model, etc.). Furthermore, the resultant states must be defined at every blade station; and these states have little physical significance.

What we propose in this paper is a new, finite-state model of rotor unsteady aerodynamics. The model is formulated purely as an induced-flow feedback, as depicted in Fig. 1. Therefore, it takes as input whatever circulatory lift distribution is present (regardless of the source). The model is based on actuator-disc theory, but modified so as to be unsteady and to have a finite number of blades. The states of the model are the coefficients of azimuthal harmonics and of radial shape functions that describe the induced-flow field. The number of functions is decided by the user. These states obey ordinary differential equations that may be written in the time or frequency domain. Therefore, the model is well-suited to aeroelastic analysis.

Theoretical Development

Potential-Flow Theory

The fundamental fluid-mechanics of this model is based on the potential-flow functions derived by Prandtl and applied by Kinner, Ref. 20. Prandtl was able, by the use of ellipsoidal coordinates, to obtain closed-form potential functions that give an arbitrary pressure discontinuity across a circular disc (an acceleration potential). Mangler and Squire, Ref. 21, and Joglekar and Loewy, Ref. 22, applied this as a steady actuator-disc theory to give induced-flow distributions in forward flight. To do this, they spread the blade loads evenly over the azimuth (i.e., an infinite number of blades). Pitt and Peters, Ref. 23, extended this work to make it an unsteady dynamic-inflow theory in the time domain. Later, Peters and Gaonkar, Ref. 24, applied higher-harmonic versions to rotors with finite numbers of blades; but the results seemed contradictory, and higher-harmonic versions were abandoned. Here, we return to a higher-harmonic theory of dynamic inflow as the basis for our unsteady model. The theory is based on the Prandtl potential function, but the pressure distribution is allowed to contain the pressure spikes of individual blades as they rotate around the disc.

The Prandtl potential function $\Phi(\nu, \eta, \bar{\psi}, \bar{t})$, can be placed in the following form

$$\Phi = \sum_{\substack{n,m \\ n>m,\ n+m \text{ odd}}} P_n^m(\nu) Q_n^m(i\eta)[C_n^m \cos(m\bar{\psi}) + D_n^m \sin(m\bar{\psi})] \tag{9}$$

where the coefficients C_n^m and D_n^m uniquely define the pressure field. The variables ν and η are ellipsoidal coordinates. On the disc, $\eta = 0$ and $\nu = \sqrt{1 - r^2}$. The functions $P_n^m(\nu)$ and $Q_n^m(i\eta)$ are Legendre Functions of the first and second kind, Refs. 26 and 27.

An important point is that Φ has a discontinuity across the disc. It follows that the pressure on the rotor disc is the difference between the upper and lower pressure. Thus, we have

$$\phi(r, \psi, \bar{t}) = -2 \sum_{n,m} P_n^m(\nu) Q_n^m(i0)[C_n^m \cos(m\psi) + D_n^m \sin(m\psi)] \tag{10a}$$

or

$$\phi(r, \psi, \bar{t}) = \sum_{n,m} \bar{P}_n^m(\nu)[\tau_n^{mc} \cos(m\psi) + \tau_n^{ms} \sin(m\psi)] \tag{10b}$$

where

$$\tau_n^{mc} = (-1)^{m+1} 2 Q_n^m(i0) C_n^m \rho_n^m \tag{10c}$$

$$\tau_n^{ms} = (-1)^{m+1} 2 Q_n^m(i0) D_n^m \rho_n^m \tag{10d}$$

In the model of this paper, this pressure distribution may vary with time. Therefore, the coefficients C_n^m, D_n^m, and τ_n^m are also time dependent.

There are two methods whereby Eq. (10b) can yield the unsteady velocity field. In the first method, we assume that ϕ oscillates harmonically (all pressures in phase) as $\phi = \bar{\phi}\exp(i\omega t)$. This is done in Refs. (23) and (25) and results in Theodorsen type integrals for $A(k)$. However, it is also possible to avoid the frequency domain and to stay entirely in the time domain for the induced flow computation. In particular, we separate the potential function (i.e., nondimensional pressure) into the part due to acceleration (Φ^A, ϕ^A) and the part due to momentum flux (Φ^V, ϕ^V). From the momentum and continuity equations, it follows that Φ^A and Φ^V must each satisfy Laplace's equation and that the flow w relates to Φ in the following ways

$$w = -\frac{1}{V}\int_0^\infty \frac{\partial \Phi^V}{\partial z}\, d\xi \equiv L[\phi^V] \tag{11a}$$

$$\overset{*}{w} = -\left.\frac{\partial \Phi^A}{\partial z}\right|_{\xi = 0} \equiv C[\phi^A] \tag{11b}$$

where V is the normalized free-stream velocity (velocity divided by ΩR), z is the coordinate normal to the rotor (positive down), and ξ is the stream-line coordinate (zero at the disc, positive upstream).

Equation (11) defines the linear operators $L[\ ]$ and $C[\ ]$. In other words, because w and $\overset{*}{w}$ can be obtained from a linear operation or Φ^V and Φ^A, and because Φ is linearly related to ϕ through the coefficients of the Legendre functions in Eqs. (9) and (10), the mathematical manipulations in Eqs. (11a) and (11b) can be treated as linear operators. It follows that, if we can invert the operators $L[\ ]$ and $C[\ ]$, then we can write a differential equation for the induced velocity at the rotor disc in terms of the pressure rise across the disk.

$$C^{-1}[\overset{*}{w}] + L^{-1}[w] = \phi^A + \phi^V \equiv \phi \tag{12}$$

Equation (12) is a time-domain induced-flow theory that provides for the evolution of induced flow given rotor lift.

Matrix Form

As it turns out, the operators in Eqs. (11) and (12) are fairly easily inverted, provided that w and ϕ are expanded in series of suitable functions. We have already seen that the potential function Φ is naturally expanded in a double series of Legendre functions and harmonic functions with coefficients C_n^m and D_n^m (or τ_n^m); and these are directly related to the pressure on the disc, Eqs. (9–10). In the same manner, we may expand the induced flow distribution (at the rotor disc) in terms of harmonics and arbitrary radial functions, $\psi_s^m(\nu)$.

$$w(r, \psi) = \sum_{n,m} \psi_s^m(\nu)[\alpha_n^m \cos(m\psi) + \beta_n^m \sin(m\psi)] \quad (13)$$

The coefficients $\alpha_n^m(\bar{t})$ and $\beta_n^m(\bar{t})$ thus become the states of our model, and they have physical significance as the coefficients of assumed flow distributions.

We may substitute Eq. (13) into Eq. (12), premultiply by $\bar{P}_n^m$ and $\cos(m\psi)$ (or $\sin(m\psi)$), and integrate over the rotor disc to obtain a set of differential equations that relate the induced flow (α_n^m, β_n^m) to the pressure (τ_n^m). The α and β equations are uncoupled on the left-hand side. The α equations are in the form below, and the β equations are identical (except that there is no $m = 0$ term, and $\hat{L}^{mrc}$ becomes $\hat{L}^{mrs}$).

$$\begin{bmatrix} \ddots & & \\ & K_n^m & \\ & & \ddots \end{bmatrix} \begin{bmatrix} \ddots & & \\ & [A_{ns}^r] & \\ & & \ddots \end{bmatrix} \begin{Bmatrix} \vdots \\ \{\overset{*}{\alpha}_s^r\} \\ \vdots \end{Bmatrix} + V \begin{bmatrix} & \vdots & \\ \cdots & \hat{L}_{pn}^{rmc} & \cdots \\ & \vdots & \end{bmatrix}^{-1} \begin{bmatrix} \ddots & & \\ & [B_{ns}^r] & \\ & & \ddots \end{bmatrix} \begin{Bmatrix} \vdots \\ \{\alpha_s^r\} \\ \vdots \end{Bmatrix} = \begin{Bmatrix} \vdots \\ \frac{1}{2}\{\tau_n^{mc}\} \\ \vdots \end{Bmatrix} \quad (14a)$$

or

$$[M]\{\overset{*}{\alpha}_s^r\} + [L^c]^{-1}\{\alpha_s^r\} = \{\tau_n^{mc}/2\} \quad (14b)$$

Note that, in Eqs. (14a) and (14b), the superscripts r and m refer to a partition number (row or column) that corresponds to a harmonic number (0 to M for cosine, 1 to M for sine). The subscripts (n, p, s) correspond to row-column indices with each partition; and they imply a certain polynomial number (e.g., $\bar{P}_n^m$, $\bar{P}_p^r$, or $\bar{\psi}_s^r$). Recall that $n > m$ and $n + m$ is odd. Therefore, (n, p, s) do not take on consecutive integers (1, 2, 3, 4, . . . etc.) as in a normal matrix index. Instead, they take on values of ($m + 1$, $m + 3$, $m + 5$, etc.). With these provisos, Eq. (14) obeys the normal rules for multiplication of partitioned matrices.

It is useful, here, to explain each of the matrix elements of Eq. (14). First, the diagonal matrix K_n^m results from the η derivative which is taken in the $C[\ ]$ operator.

$$K_n^m = \frac{-Q_n^m(i0)}{iQ_n^m(i0)'} = \frac{2}{\pi} H_n^m \quad (15a)$$

where

$$H_n^m = \frac{(n+m-1)!!(n-m-1)!!}{(n+m)!!(n-m)!!} \quad (15b)$$

The double factorial symbol, ( )!!, implies a factorial which takes on only every other term down to 2 or 1 [$n!! = n(n-2)(n-4) \ldots (2 \text{ or } 1)$].* By the use of the gamma function, one can show that $(0)!! = 1$, $(-1)!! = 1$, and $(-3)!! = -1$. Due to the ratios of double factorials in Eq. (15), H_n^m and K_n^m are very well conditioned, despite the fact that the individual factorials can become quite large.

*See Ref. 26 page xliii or Ref. 27, pages 258 and 1046.

The matrices $[A^m]$ and $[B^m]$ provide for coupling between radial inflow distributions of any given harmonic. They are simple integrals of the Legendre functions and of the assumed functions.

$$A_{ps}^m = \int_0^1 \bar{P}_p^m(\nu)\psi_s^m(\nu)\nu d\nu \quad (16a)$$

$$B_{ps}^m = \int_0^1 \bar{P}_p^m(\nu)\psi_s^m(\nu)d\nu \quad (16b)$$

We recall that on the disc, $\bar{r} = \sqrt{1-\nu^2}$, $\nu = \sqrt{1-\bar{r}^2}$, and $-\nu d\nu = \bar{r}d\bar{r}$. Thus, the integrals can be performed in either $\bar{r}$ or ν.

The matrix $\hat{L}$ contains the interharmonic coupling of the model. It gives the pth polynomial of the rth harmonic of induced flow due to the nth polynomial of the mth harmonic of pressure. Mathematically, this is

$$\hat{L}_{pn}^{omc} = \frac{1}{2\pi}\int_0^{2\pi}\int_0^1 \bar{P}_p^o(\nu_0)\int_0^\infty \frac{d}{dz}[\bar{P}_n^m(\nu)\bar{Q}_n^m(i\eta)] \times \cos(m\psi)d\xi\, d\nu_0 d\psi \quad (17a)$$

$$\hat{L}_{pn}^{rmc} = \frac{1}{\pi}\int_0^{2\pi}\int_0^1 \bar{P}_p^r(\nu_0)\cos(r\psi_0)\int_0^\infty \frac{d}{dz} \times [\bar{P}_n^m(\nu)\bar{Q}_n^m(i\eta)]\cos(m\psi)d\xi\, d\nu_0 d\psi_0 \quad (17b)$$

$$\hat{L}_{pn}^{rms} = \frac{1}{\pi}\int_0^{2\pi}\int_0^1 \bar{P}_p^r(\nu_0)\sin(r\psi_0)\int_0^\infty \frac{d}{dz} \times [\bar{P}_n^m(\nu)\bar{Q}_n^m(i\eta)]\sin(m\psi)d\xi\, d\nu_0 d\psi_0 \quad (17c)$$

where the Legendre functions have been normalized and where ξ begins at the point ν_0, ψ_0 on the disc and extends along a streamline. Thus, ν, η, and $\bar{\psi}$ depend on the value of the ξ coordinate as well as its point of origin on the disc. For axial flow, $\xi = -z$, and the $\hat{L}$ matrices become identity matrices. The V outside of $\hat{L}$ is the free-stream velocity divided by ΩR. It follows that $\hat{L}$ depends only on the disc angle of attack. The d/dz in Eq. (17) must be transformed to η and ν derivatives through the chain rule; and, then, the $\hat{L}$ elements can be found numerically, as outlined in Ref. 28. However, subsequent to the publication of Ref. 28, we have been able to obtain these integrals in closed form. They depend only on wake skew angle, α, and are given in Ref. 35.

Pressure Integrals

In order to apply the above theory, we must be able to write the pressure coefficients, τ_n^m, in terms of circulatory blade lift. We assume nothing about this blade lift except that it occurs only on the blade and is available at every instant of time from a blade-lift model (e.g., dynamic stall, linear lift-curve slope, quasi-steady, etc.). At that instant of time, we may expand this lift distribution as a discontinuous pressure distribution in terms of the Legendre functions and harmonics.

For example, the cosine harmonics are

$$\tau_n^{mc} = \frac{1}{\pi}\sum_{q=1}^{Q}\int_0^1\int_{-\bar{b}}^{+\bar{b}} P_q(\bar{r}, y, t)\bar{P}_n^m(\nu)\cos(m\psi)\frac{1}{\nu}d\bar{r}dy \quad (18)$$

where $d\nu d\psi$ has been expressed as $-\frac{1}{\nu}d\bar{r}dy$ on each blade (at ψ_q). If a particular blade theory does not provide chordwise pressure, we may assume some appropriate distribution $P_y(y)$, which gives P_q in terms of lift per unit length, L_{cq}.

$$P_q(\bar{r}, y, \bar{t}) = L_{cq}(\bar{r}, \bar{t})P_y(y)/\int_{-\bar{b}}^{+\bar{b}} P_y(y)dy$$

The chordwise part of the integral may then be expressed in closed form, f_m, to yield the fundamental τ_n^m equations.

$$\tau_n^{oc} = \frac{1}{2\pi}\sum_{q=1}^{Q}\int_0^1 L_{cq}(\bar{r}, t)f_m\bar{P}_n^o(\nu)\frac{1}{\nu}\,d\bar{r} \qquad (20a)$$

$$\tau_n^{mc} = \frac{1}{\pi}\sum_{q=1}^{Q}\int_0^1 L_{cq}(\bar{r}, t)f_m\bar{P}_n^m(\nu)\frac{1}{\nu}\,d\bar{r}\cos(m\psi_q) \qquad (20b)$$

$$\tau_n^{ms} = \frac{1}{\pi}\sum_{q=1}^{Q}\int_0^1 L_{cq}(\bar{r}, t)f_m\bar{P}_n^m(\nu)\frac{1}{\nu}\,d\bar{r}\sin(m\psi_q) \qquad (20c)$$

(Note that $\tau_1^{oc} = \sqrt{3/2}\,\delta C_T$, $\tau_2^{1s} = -\sqrt{15/2}\,\delta C_L$, and $\tau_2^{1c} = -\sqrt{15/2}\,\delta C_M$).

The functions, f_m, which appear in Eq. (20), are given by

$$f_m = \frac{\int_{-\bar{b}}^{+\bar{b}} P_y(y)\exp(myi/\bar{r})dy}{\int_{-\bar{b}}^{+\bar{b}} P_y(y)dy} \qquad (21)$$

where the complex nature of f_m implies a coupling between $\sin(m\psi_q)$ and $\cos(m\psi_q)$ in the usual way.

Application Considerations

Choice of Correction Functions

From Eq. (21), we see that f_m is only a function of $m\hat{b}/r = k_m$. For a lifting line model, all lift is concentrated at $y = 0$; and, therefore, $f_m = 1$. For uniform pressure over the chord, we have $f_m = \sin(k_m)/k_m$. (Reference 28 outlines other possible cases for f_m.) Strictly speaking, a theory with $f_m = 1$ for all harmonics (a lifting line at the point of velocity computation) does not converge as the number of harmonics increases without bound. This is to be expected, since it is well-known that lifting-line theory has a singular integral, Ref. 29. Nevertheless, for realistic helicopter parameters and $m < 30$, we find that $f_m = 1$ is numerically accurate. Therefore, one may reasonably take $f_m = 1$ with little loss of accuracy. On the other hand, if one wishes to include more than 30 harmonics, the choice $f_m = \sin(k_m)/k_m$ converges well and effectively filters out the effect of bound vorticity from the computation.

Another correction factor that can be applied to the model is the mass-flow parameter V in Eq. (14a). Strictly speaking, this is the normalized free-stream velocity ($\sqrt{\mu^2 + \lambda^2}$) in a theory that assumes that induced flow is a small perturbation to V. However, from momentum considerations, one can extend V to include also a steady induced flow about which the induced flow in Eq. (14a) is perturbed, Ref. 30. The extended V is given by

$$V = \frac{\mu^2 + (\lambda + \bar{\nu})(\lambda + 2\bar{\nu})}{\sqrt{\mu^2 + (\lambda + \bar{\nu})^2}} \qquad (22)$$

where $\bar{\nu}$ is the momentum-theory value of the average induced flow that obeys the relationship.

$$\overline{C}_T = 2\bar{\nu}\sqrt{\mu^2 + (\lambda + \nu)^2} \qquad (23)$$

Thus, Eq. (22) allows for the added energy in the flow and offers a smooth transition from hover to forward flight.

Furthermore, Ref. 30 shows that the steady and perturbation thrust (as well as the steady and perturbation induced flow) can be combined to obtain a nonlinear induced flow model that is not a perturbation theory. To do this, one first assumes that all quantities in Eq. (14a) are total quantities. Second, one allows V of Eq. (22) to multiply all rows of $[\hat{L}]^{-1}$ except the first row. For the first row, one multiplies by V_T, where

$$V_T \equiv \sqrt{\mu^2 + (\lambda + \bar{\nu})^2} \qquad (24)$$

Third, instead of Eq. (23), one takes $\bar{\nu}$ in V and V_T from the instantaneous value of induced flow, w, characterized by the α_n^m coefficients.

$$\bar{\nu} = \frac{2}{\sqrt{3}}\langle 1000\ldots 0\rangle\,[\hat{L}_{ln}^{rmc}]^{-1}\begin{bmatrix}\ddots & & \\ & B_{lp}^r & \\ & & \ddots\end{bmatrix}\{\alpha_p^r\} \qquad (25)$$

This makes the model a nonlinear theory of induced flow since V and V_T in Eq. (14a) will depend upon α_p^r. (The approximations $\bar{\nu} = \overline{C}_T/(2V_T) = \tau_1^{oc}/(\sqrt{3}V_T) \simeq \sqrt{3}\,\alpha_1^0$ are also useful).

One could also entertain corrections for ground effect or fuselage interference, Ref. 29. However, no correction is needed for the tip-loss effect. Tip losses are implicit in the model since it gives the three-dimensional flow.

Choice of Model Texture and Expansion Functions

The above theory offers a number of choices for the user, and these afford a great deal of flexibility in the model. Of primary importance is the number of harmonics and the number of radial functions for each harmonic. Here, the texture of the aerodynamic model should match the texture of the dynamic model. For example, if the dynamic model includes modes through a certain frequency range, then enough harmonics should be kept to ensure that aerodynamic terms are present for the frequencies of interest. Similarly, if a certain number of radial modes are present in the dynamic model, then a corresponding number of radial inflow distributions should be used to ensure that all modes have the correct induced-flow feedback.

Another important choice is that of the type of functions to be used for ψ_s^m in Eq. (13). These functions should be linearly independent and well conditioned, the latter implying some type of orthogonality. The best choice is $\psi_s^m = \frac{1}{\nu}\bar{P}_n^m(\nu)$, the functions which also appear in the τ_n^m integrals, Eq. (20). These functions have several exceptional characteristics that make them the best choice. First, they are simple polynominals in $\bar{r}$. The first function (or polynominal) for each harmonic (m) is a constant times $\bar{r}^m$

$$\frac{1}{\nu}\bar{P}_{m+1}^m(\nu) = \sqrt{(2m+3)!!/(2m)!!}\,\bar{r}^m \qquad (26)$$

The higher-numbered polynomials for each harmonic ($n = m + 1$, $m + 3$, $m + 5$, etc.) simply add another odd or even power of r for each term ($\bar{r}^m$, $\bar{r}^{m+2}$, $\bar{r}^{m+4}$, etc.). This implies that the first term in each harmonic is directly related to the "uncorrected" dynamic inflow model of Ref. 23 with the change of variable

$$\alpha_{m+1}^m = \rho_{m+1}^m\lambda_{mc}/\sqrt{(2m+1)} \qquad (27a)$$

$$\beta_{m+1}^m = \rho_{m+1}^m\lambda_{ms}/\sqrt{(2m+1)} \qquad (27b)$$

Thus, the present theory includes dynamic inflow as the first term of each harmonic. Another advantage of this choice of $\psi_n^m = \frac{1}{\nu}\bar{P}_n^m(\nu)$ is in the computation of both $[A^m]$ and $[B^m]$. The matrix $[A^m]$ reduces to identity for this case; and $[B^m]$ can be obtained in closed form along with its inverse, $[\bar{A}^m] \equiv [\bar{B}^m]^{-1}$ (Ref. 35). All of our numerical work to date verifies that this is the most logical choice for expansion functions. The authors also have a subroutine, available to the public, that can efficiently calculate $P_n^m(\nu)/\nu$ for m and n into the 1,000's.

Another application issue is that, in some problems, it may be inconvenient to perform the integrals of L_{cq} required to obtain the τ_n^m forcing terms. If, however, one has chosen the same number of (or fewer expansion) terms S as there are radial modes for vertical blade bending, then τ_n^m can be obtained from the generalized forces already being used for structural response, as outlined in Ref. 28. It follows that the present model can be applied in either the modal or finite-element arena.

Two-Dimensional Approximation

As a final aspect of application issues, we should mention the possibility of a two-dimensional approximation (based on our general theory) that could be used in a blade-element, hover application. Although we do not recommend the use of our model in this way, such a formulation is useful for purposes of comparison both with Loewy theory and with the two-dimensional version of Miller theory, Eqs. (5)–(8). To formulate such a model, one must prescribe both a single radial distribution of inflow for each harmonic

$$\Psi^m(r) = \sum_n a_n^m \frac{1}{\nu} P_n^m(\nu) \tag{28a}$$

and a weighting function

$$\Lambda^m(r) = \sum_n b_n^m \frac{1}{\nu} P_n(\nu) \tag{28b}$$

Substitution into Eq. (14) for the case of hover gives induced flow equations for each harmonic independent of r (i.e., of ν),

$$T_m \overset{*}{\lambda}{}_I^m + V\lambda_I^m = \frac{1}{2\pi} \sum_{q=1}^{Q} [L_{cq}(r)/r] f_m \cos(m\psi_q) \tag{29a}$$

The elements, T_m, are the time constants of each harmonic in this two-dimensional approximation; and they are given by

$$T_m = \{b_n^m\}^T \begin{bmatrix} \ddots & & \\ & K_n^m & \\ & & \ddots \end{bmatrix} \{a_n^m\} / \{\bar{b}_n^m\}^T \{a_n^m\}$$

$$m = 0, 1, 2, \ldots \tag{29b}$$

Although T_m depends upon the choice of Ψ^m and Λ^m used in the two-dimensional approximation, this dependence is not strong; and Ref. (28) offers a formula which gives an average value of T_m for a family of assumptions

$$T_m = \frac{2}{\pi} \sqrt{\frac{2}{m + t + 4}\,\frac{(2m)!!}{(2m+1)!!}}$$

$$\simeq \left. \frac{\sqrt{2/\pi}}{m + t/2 + 19/8} \right|_{\text{large } m} \tag{30}$$

where t is the power of $\bar{r}$ in the assumed pressure or velocity. By comparison, the eigenvalues of $[\bar{B}^m]^{-1}\,[K_n^m]$ give time constants

$$T_m = \frac{3/4}{m + 3/2} \tag{31}$$

which are the maximum possible values.

Table I gives a comparison of T_m as computed from the eigenvalues, from a uniform pressure/velocity assumption ($t = 0$), and from the Pitt model of Ref. (23) ($t = m$). One can see that the $t = 0$ results are close to the eigenvalues of the system for all m, but the Pitt model deviates at larger values of m. Identified values of T_1 in Refs. (31–32) and of T_0 in Ref. (33) verify the reasonableness of this two-dimensional approximation.

Connection Between Present Theory and Classical Theories

Present Model in Axial Flow

In order to compare the above theory with the existing classical theory from Ref. 2, we consider the actuator-disc equations for the special case of a non-lifting climb ($V = \lambda =$ climb rate), which is the Loewy assumption. If we further assume a linear, blade-element lifting theory

$$L_{cq} = a\bar{c}(\Theta_q \bar{r}^2 - \lambda_I \bar{r})/2 \tag{32}$$

then we can solve for λ_I and L_{cq} in closed form from Eqs. (29) and (32). The result is a lift-deficiency function in the form of Eq. (3) with the inflow feedback given by

$$A(k) = \frac{\sigma a}{8} \sum_{j=-J}^{J} \frac{f_m(k_m)}{V + T_m(\omega - jQ)i} \tag{33}$$

where Q is the number of blades, ω is the frequency in the nonrotating reference frame, k_m is the reduced frequency of the mth harmonic ($m\hat{b}$), and m is a harmonic number that specifies the inflow harmonic being excited by jQ.

The derivation of Eq. (33) is too lengthy to be repeated here. However, it is completely straightforward and is done entirely in closed form with no added assumptions. The relationship between m and j follows directly from the derivation and is closely related to the relationship between rotating and nonrotating frequency. This relationship is outlined in Table II. We note that the differential mode is only present for even-bladed rotors, and higher-harmonic cyclic is only present for rotors with a sufficient number of blades ($s < Q/2$).

Near-Wake Expansion of Loewy/Miller Theory

We wish to compare the near-wake approximation of lift deficiency for the theories in Refs. 2 and 3, with the present model, Eq. (33). For clarity, we recall that the W function, as given in Eq. (7) of Ref. 2, depends explicitly on the phase between the pitch of different blades. As it turns out, the W function for any particular type of excitation (collective, cyclic, or differential) can be expressed as in our Eq. (6), with k given by $\hat{b}\omega_R$ and with ω_R given from Table II.

Thus, Eqs. (6) and (8) can be compared with Eq. (33) to determine the relationships between the two theories. At first glance, the only correlation between the formulas seems to be that ω and ω_R related in a similar manner to m and j for each

Table I Time constants (T_m) for two-dimensional inflow approximation, mth harmonic

m	Eigenvalue	Uniform Pressure/ Velocity	Ref. (23)
0	.500	.458	.424
1	.300	.268	.226
2	.214	.196	.155
3	.167	.156	.118
4	.136	.129	.096
∞	.750/m	.798/m	.564/m

Table II Harmonic relationships

Type of Mode	Rotating Frequency	Inflow Harmonic	Phase Shift of qth Blade
Collective	$\omega_R = \omega$	$m = \|jQ\|$	0
Regressing Cyclic (s-th harmonic)	$\omega_R = \omega + s$	$m = \|jQ + s\|$	exp (is ψ_q)
Progressing Cyclic (s-th harmonic)	$\omega_R = \omega - s$	$m = \|jQ - s\|$	exp ($-$is ψ_q)
Differential	$\omega_R = \omega \pm Q/2$	$m = \|jQ \pm Q/2\|$	$(-1)^{q+1}$

type of mode. In truth, however, the formulas are nearly identical. To see this clearly, we expand the function $A = \pi k(1/2 + W)$ in terms of its complex ω poles, $\omega = mQ + (Vk/\bar{b})i$,

$$A(k) = \pi k(1/2 + W)$$

$$= \frac{\sigma a}{8} \sum_{j=-\infty}^{+\infty} \frac{1}{V + (\bar{b}/k)(\omega - jQ)i} \quad (34)$$

where we have used $a = 2\pi$, $h = 4V/\sigma$, and $\sigma = 2\bar{b}Q/\pi$.

Comparison of Lift-Deficiency Functions

We can now directly compare the two theories: near-wake Loewy (or Miller), Eq. (34); and our state-space model, Eq. (33). The similarities between these two equations are amazing when one considers that the former is a closed-form, actuator-disc model and the latter is a vortex-layer model. To begin, we look at the differences. Of course, our present theory is a truncated model. It has only a finite number of states, $2J + 1$. Therefore, its correlation with Loewy/Miller theory will depend on the convergence characteristics of the series in Eq. (33). Next, we note that either representation has a real part V and an imaginary part $(\omega - jQ)i$ in the denominator of each term. However, in Loewy theory, this latter term multiplies a fixed number, $\bar{b}/k$, that depends only on reduced frequency; whereas, in the present theory, this imaginary term multiplies T_m, which depends on the summation index in the series. Therefore, Eq. (33) must rely on the numerator terms, $f_m(k_m)$, for formal convergence. However, in practice, even with $f_m = 1$, the divergence is very slow. Therefore, as long as no more than 20 to 30 terms are used ($k < .6$), Eq. (33) is essentially stable and does not diverge, even with $f_m = 1$.

Given that Eq. (33) converges (either through f_m or truncation), we now turn to how well it compares with Eq. (34). The key to this is the understanding that both series are dominated by the pole that places ω closest to jQ (and, therefore, ω_R closest to m). Near that pole, we may replace $\bar{b}/k$ by

$$\bar{b}/k = \bar{b}/(\bar{b}|\omega_R|/r) = r/m = T_m \text{ (Loewy)} \quad (35)$$

Eq. (35) gives us the time constants from Loewy theory, and these can be compared with those from our theory, Eqs. (30) and (31). If we take Eq. (35) at the 75 percent to 80 percent radial location, then the time constants from the two theories are nearly identical for large m, Table I at $m = \infty$. However, for smaller m, the theories begin to deviate. At $m = 1$, a point for which the actuator-disc time constant is well established by parameter identification as .22 – .24 (Refs. 31–33), Loewy theory gives three times the correct apparent mass. Similarly, work in Ref. 29 establishes T_0 at .42, but the Loewy theory gives $T_0 = \infty$. The source of this overprediction is that Ref. 2 is based on a two-dimensional assumption; but the apparent-mass time constant is a three-dimensional effect.

Therefore, not only does our new theory essentially recover Loewy theory as a special case, but it actually improves Loewy theory through a better estimate of apparent mass at small m. It further follows that any analysis that now uses Loewy theory could improve that theory by replacement of $k = \bar{b}|\omega_R|$ by $k = \bar{b}(\omega_R + 1.5)$, Eq. (31). This would give the theory finite apparent mass at $\omega = 0$ and would give more realistic values of apparent mass at other frequencies.

Comparison with Theodorsen Theory

The next area of investigation is the correspondence of our theory with Theodorsen Theory, which is the limit as h (or V) goes to ∞. For Loewy theory, W clearly goes to 0 in this case; and A approaches $\pi k/2$, the Theodorsen near-wake approximation. It would seem that this limit would be unapproachable by our new theory because Eq. (34) shows that $V = \infty$ will give $A = 0$ for a finite number of terms. However, recognizing that our series is essentially the same as the Loewy expansion, Eq. (34), Ref. 28 shows that, in the limit as many terms are taken, our theory will similarly recover the near-wake approximation to the Theodorsen theory for $V = \infty$. The number of terms required for convergence is

$$JQ/m >> V \quad (36)$$

Equation (36) implies that the ratio of harmonics retained to harmonics desired must be greater that $10 \times V$ (for 10 percent error).

Of course, the above limit as $J \to \infty$ assumes that one takes an appropriate f_m that allows formal convergence. However, for typical helicopter problems ($V < 0.1$, $m = Q = 4$), only four harmonics would be needed to capture the contribution of the near-wake value ($\pi k/2$) to the total solution.

Two-Dimensional Airfoil Theory

Although we believe that Eq. (34) will find its broadest applications in the range of rotor dynamic problems with frequencies less than 30/rev, it is important to realize that the theory is not restricted to this. For example, if one takes $f_m = J_0(k_m) - i\,J_1(k_m)$, which corresponds to the pressure distribution for a flat-plate airfoil, then the theory will converge to the induced velocity that gives non-penetration of the airfoil surface. For example, Fig. 2 shows the velocity distribution in the vicinity of the blade at 1,000 harmonics for a normalized blade pitch (on the blade, we have $-1 < y/\bar{b} < +1$). The figure shows the large upwash at the leading edge (negative w) and the convergence to nonpenetration ($w = 2.44$) on the blade surface. Of course, this convergence is slow because 1,000 harmonics around the azimuth implies only 16 harmonics across the chord for $\bar{b} = .05$. Therefore, the present theory is slow to converge on the induced flow near the blade surface, where the effects of concentrated bound vorticity is large. However, normally the effect of bound vorticity is included in the lift model and is not desired in the inflow model. For such cases, our theory with $m < 30$ is ideal. It provides an accurate representation of the induced flow from the shed wake, while filtering out the effect of bound vorticity.

Prandtl-Goldstein Three-Dimensional Effects

In the above discussion, we have concentrated on comparisons of two-dimensional theories with a two-dimensional approximation to our model in axial flow. We now turn to comparison with three-dimensional models for lightly loaded rotors in axial flow. Prandtl offers an approximation for static inflow based on a flat-wake assumption, and Goldstein provides a more accurate helical-wake solution, Ref. 34. These solutions are provided in terms of a momentum-correction factor, F; and they are virtually identical for $\lambda/Q < 0.1$, which is the case for most helicopters. In essence, the factor F forces the induced flow to become larger near the tip so that the angle of attack and lift will approach zero as $\bar{r}$ approaches unity. Figure 3 shows that the solution for our model ($M = 4$ harmonics and

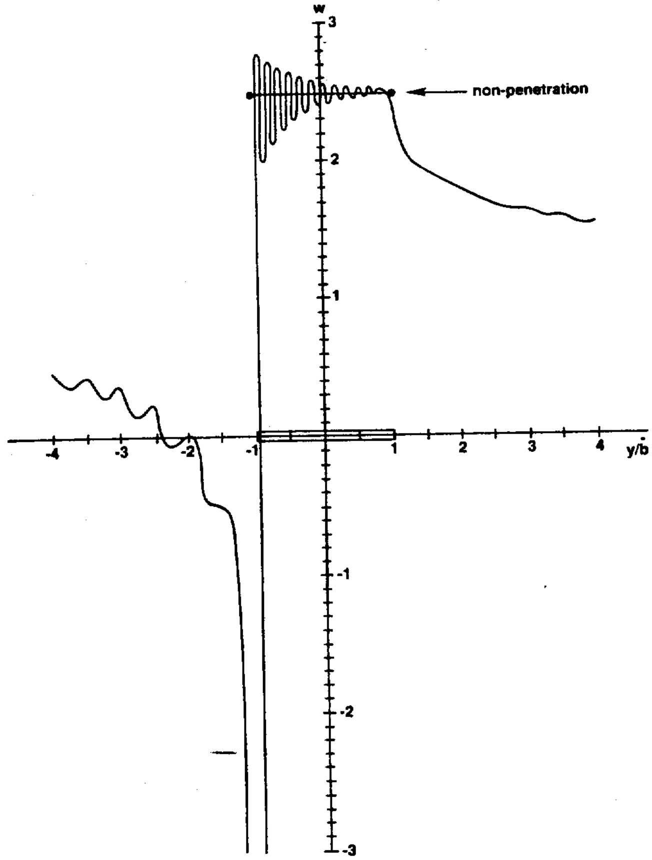

Fig. 2. Velocity distribution near a flat-plate airfoil, $f_m = J_0(m\hat{b}) - i\,J_1(m\hat{b})$, 1000 harmonics, $\omega = 0$.

$S = 4$ polynomials, 36 state variables) is very close to the Prandtl/Goldstein solution. Numerical results have shown that our model does converge to the Prandtl/Goldstein lift with 4 percent error at 10 state variables, 2 percent error at 25 state variables, and 1 percent error at 50 state variables. Thus, three-dimensional wake effects are implicit in this model.

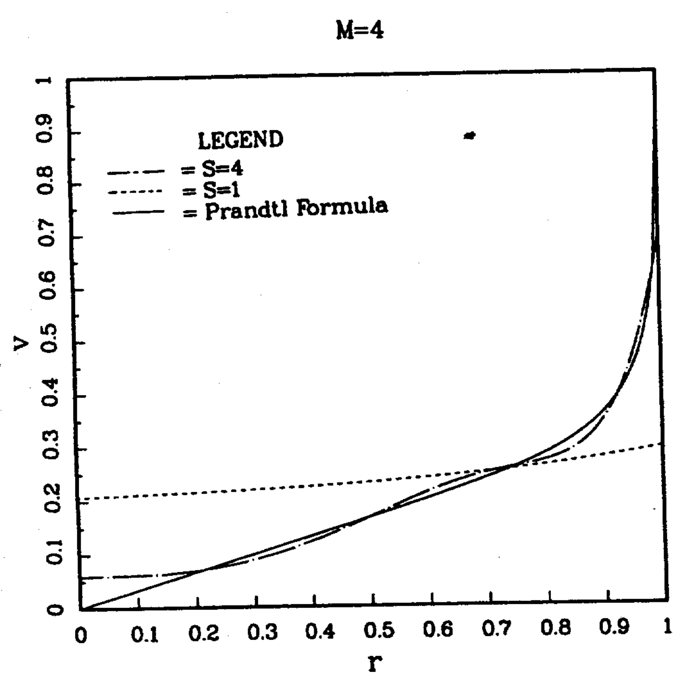

Fig. 3. Radial induced-flow distribution, one blade, 4 harmonics, $\sigma a = 0.20$, $V = \bar{\lambda}$ .05, $Q = 4$, $\omega = 0$.

Numerical Results

Lift-Deficiency

In Ref. 35, we have given detailed comparisons between the near-wake Loewy approximation and the two-dimensional version of our model in hover. Those results show that: 1) the two theories agree at higher frequencies ($\omega > 4$), 2) Loewy theory is in error at low frequencies ($\omega < 1$) due to the overly large Loewy apparent mass terms and, 3) the number of terms required to converge numerically to the near wake theory at $\omega = m$ is $JQ/m > 10V$, as predicted by analysis. However, what is left unanswered in that paper is how our new theory compares with the complete Loewy theory (including the Bessel functions J_n and Y_n which are dominated by terms of type *klnk* at small *k*).

In Figs. 4–7, we compare lift-deficiency functions from the Loewy near-wake theory ($A = \pi k/2 + \pi kW$), from the full Loewy theory, from our theory with $J = 3$ ($JQ = 12$ harmonics), and from our theory with $J = 6$ ($JQ = 24$ harmonics). All results are for $Q = 4$, $V = .05$, and $\sigma = 0.61$. A comparison of the two Loewy theories gives an indication of the importance of the *klnk* type terms. A comparison of Peters' theory for $J = 3$ and $J = 6$ indicates how our theory implicitly captures the *klnk* terms as J increases. However, it is important to realize that we do not expect our theory to converge to Loewy theory. The Loewy theory is only a two-dimensional approximation; while our theory is based on a three-dimensional model. Thus, just as Loewy theory over-estimates the apparent mass terms at integer ω's, it over-estimates the effect of these *klnk* terms due to its model of infinite wake sheets (as opposed to a truly returning wake).

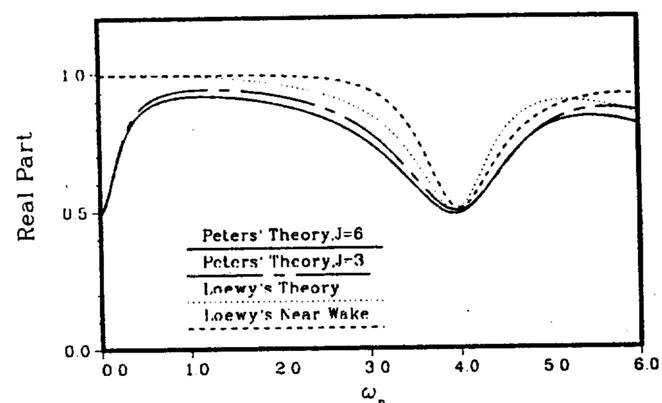

Fig. 4a. Real part of lift-deficiency function, collective mode, $V = .05$, $Q = 4$, $J = .061$, $a = 2\pi$.

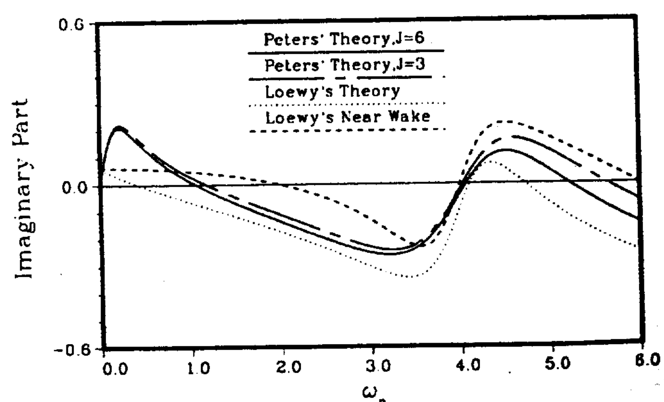

Fig. 4b. Imaginary part of lift-deficiency function, collective mode, $V = .05$, $Q = 4$, $J = .061$, $a = 2\pi$.

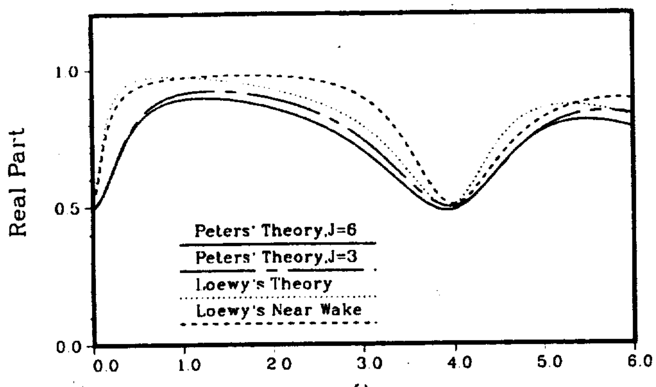

Fig. 5a. Real part of lift-deficiency function, regressing mode, $V = .05$, $Q = 4$, $J = .061$, $a = 2\pi$.

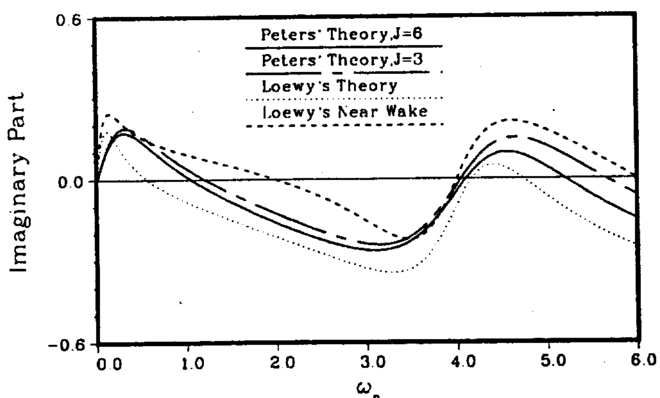

Fig. 5b. Imaginary part of lift-deficiency function, regressing mode, $V = .05$, $Q = 4$, $J = .061$, $a = 2\pi$.

Figure 4 provides a comparison of these four models for collective excitation. The real part of $C'(k)$ shows close agreement among all models at higher frequencies, and all models show the loss of lift at $\omega = 4$. However, the models exhibit a large difference near $\omega = 0$, for which our model approaches the correct (experimentally verified) deficiency, 0.5. There is little effect of the *klnk* terms, and the $J = 3$ results have converged. For the imaginary portion of $C'(k)$, the curves for $\omega < 1.0$ show a large discrepancy between Loewy theory and our theory. The slope of the Im $C'(k)$ at $\omega = 0$ is directly proportional to the time constant, T_0, for the collective mode and to T_1 for the regressing mode. Thus, the slopes of $J = 3$ and $J = 6$ curves reflect $T_0 = .458$ as in Table I. This number is also in agreement with the experimental results of Carpenter and Fridovich, Ref. 36, $T_0 = .424$. The Loewy theory, in contrast, shows an infinite mass (jump in Im $C'(k)$) and an incorrect variation with ω. Furthermore, the *klnk* terms provide a large contribution to Loewy theory but of the wrong sign to improve correlation with our theory. As we move to the frequency range $1.0 < \omega < 3.0$ (for which Loewy theory should be more accurate), we see a dramatic change in trends. In that range, the *klnk* terms of Loewy's complete theory give a large improvement in correlation between models. Thus, we conclude that *klnk* terms are important in this range ($k \approx 0.1$) and that the $J = 3$ results from our theory have implicitly captured these terms. Next, near $\omega = 4.0$, all theories show that the Im $C'(k)$ approaches zero as ω approaches this integer multiple. Lastly, for $\omega > 4.0$, we require about six times as many harmonics to converge on Im $C'(k)$ as we did for Re $C'(k)$.

The above trends are repeated for regressing and progressing excitations, Figs. 5 and 6. The Loewy theories give overly large slopes for the imaginary component at $\omega < 0.5$. The J

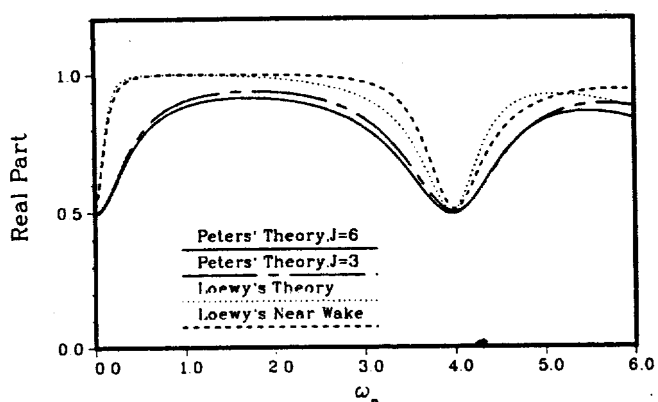

Fig. 6a. Real part of lift-deficiency function, progressing mode, $V = .05$, $Q = 4$, $J = .061$, $a = 2\pi$.

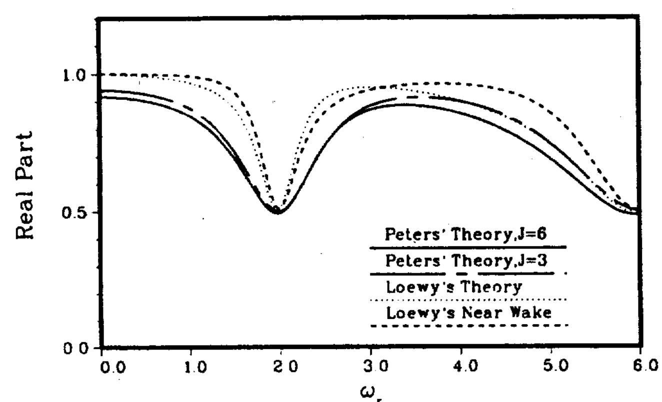

Fig. 7a. Real part of lift-deficiency function, differential mode, $V = .05$, $Q = 4$, $J = .061$, $a = 2\pi$.

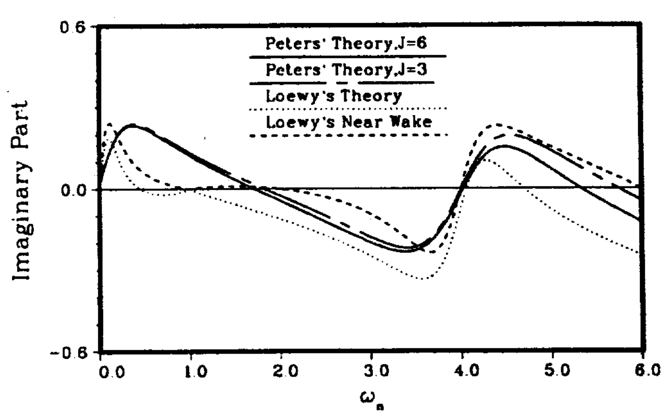

Fig. 6b. Imaginary part of lift-deficiency function, progressing mode, $V = .05$, $Q = 4$, $J = .061$, $a = 2\pi$.

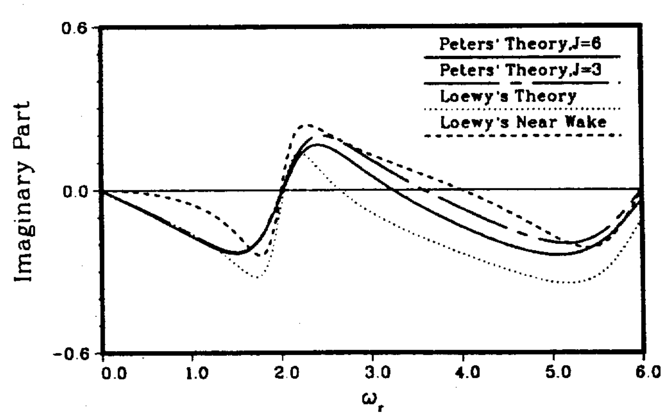

Fig. 7b. Imaginary part of lift-deficiency function, differential mode, $V = .05$, $Q = 4$, $J = .061$, $a = 2\pi$.

= 3 and J = 5 curves in Fig. 5 reflect T_1 = .268, as in Table I. This is in agreement with T_1 = .226 as measured in Ref. 37. The Loewy curve, on the other hand, gives a slope that reflects T_1 = .750, about three times too large. For larger ω, Loewy theory correlates better, provided *klnk* terms are included; and J = 3 results have converged at $\omega < 4.0$ for both real and imaginary parts. (Loewy's theory exhibits an abnormality at ω = 1 for the progressing mode because that is seen as ω_R = 0 in the rotating system). Figure 7 completes the set with $C'(k)$ for a differential excitation. The Loewy theory shows no lift deficiency at ω_R = 0 since it treats this as a static excitation. However, ω_R = 0 for a differential mode is seen by the flow as a 2/rev progressing excitation. Thus, our theory shows Re $C'(k) < 1.0$ at $\omega_R = 0$. The Im $C'(k)$ at $\omega_R < 1.0$ clearly shows the importance of the *klnk* terms and the fact that they are captured by our finite state model.

Thus, from these results, we may conclude that our finite state model not only captures Loewy theory and Theodorsen theory in hover but also improves upon them through a more accurate wake model. The number of terms required to converge on Re $C'(k)$ for $\omega = m$ is $JQ > 10Vm$, and the number of terms required for convergence to Im $C'(k)$ is approximately six times this number.

Experimental Frequency Response

There are two good sets of data on the frequency response of two-bladed rotors. The first set of data, taken from Rev. 31, is for collective excitation at zero lift ($V = h = 0$). The system parameters are $B^4\gamma = 5.35$, $\bar{p} = 1.015$ and $\sigma = .066$. Figure 8 shows the comparison of Loewy theory, actuator-disc theory, and this data at two different RPM's. The two data sets (circles and triangles) have the same fundamental flapping frequency ($\bar{p}$ = 1.015/rev) but different higher-mode frequencies. Thus, the ω at which the two data sets deviate (ω = 2.4) shows where higher modes become important. Both theories include the nonlinear V (or h) which aids correlation at ω = 2. However, this nonlinear term has negligible effect at $.2 < \omega < 1.8$. The comparisons are very instructive. Near ω = 0, the present theory shows the correct deficiency in Re(β), Fig. 8a; but the singularity in the Loewy function forces F' = 1 at ω = 0. As we approach the ω = 0.5 peak, the Loewy theory correspondingly gives an inaccurate representation, showing no peak at all. The new theory adequately matches the data.

Similarly, in the imaginary part, Fig. 8b, for $\omega < 1.0$, the new theory predicts the phase well; whereas Loewy does not. Beyond this point ($0.8 < \omega < 1.6$), both theories do a good job; but the present model is more accurate through the critical range for which we previously saw the largest differences in C' ($1.0 < \omega < 1.6$). As we approach the 2/rev cusp ($1.6 < \omega < 2.0$), the Loewy theory does better in the prediction of the Re(β); but the new theory does better on Im(β). In summary, both theories do a good job of correlation of this data for $\omega > .25$. By comparison, the theory without inflow dynamics does a poor job of matching the data near ω = 0 and for $\omega > 1.0$.

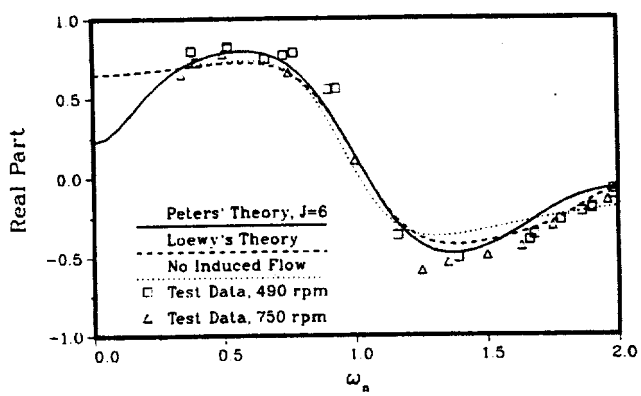

Fig. 8a. Real part of flapping response, collective mode, $Q = 2$, $B = 0.95$, $\sigma = .06b$, $\gamma = 6.63$, $V = 0$, $p = 1.015$, Ref. (30).

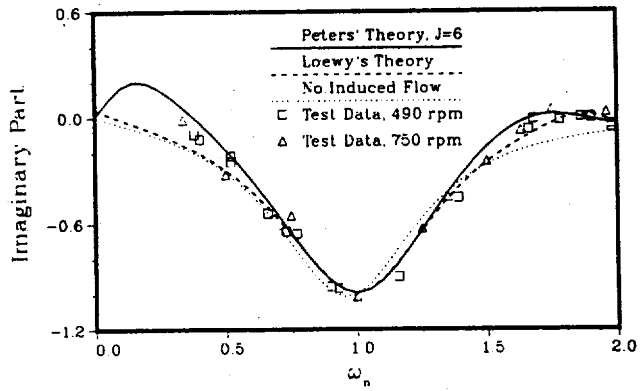

Fig. 8b. Imaginary part of flapping response, collective mode, $Q = 2$, $B = 0.95$, $\sigma = .06b$, $\gamma = 6.63$, $V = 0$, $p = 1.015$, Ref. (30).

A second set of data that is important here is the pitch-stirring experiments of Ref. 37. These data are for a two-bladed rotor that could be excited in a purely progressing or regressing mode (progressing gives $0 < \omega_R < 1$, regressing gives $\omega_R > 1$). Ref. 28 shows that this data is better correlated with our new theory than with Loewy theory.

From these data, we find that the new theory is consistently better than Loewy theory both in the physical explanation of its behavior and in comparison with frequency-response data. When we further recall that the new theory is in the time domain and is not restricted to axial flight, the new theory is a clear choice for an unsteady inflow model.

Other Correlations

We now turn to computations for which Loewy theory cannot be applied. One such case is the computation of flow off the blade in forward flight. Once we know α_n^m and β_n^m, we have the entire potential function and, consequently, the entire pressure and velocity distribution. Reference 35 provides a detailed comparison of our theory with both steady and unsteady flow measurements off the blade, as described in Ref. 32.

Another relevant computation is comparison of theory and experiment for rotor response to a ramp change in collective pitch, Ref. 36. This time-domain solution cannot be performed by classical theories. Furthermore, due to the V = 0 start-up, we must use the nonlinear version of actuator-disc theory. For this case, we use a single radial function for inflow. Furthermore, we only use a single harmonic, m = 0. Figure 9 shows the comparisons of theory and experiment. Also shown on Fig. 9 are computations from a free-wake program with curved vortex elements from Ref. 33. We note that the present theory gives good correlation both with the experiment and with the free-wake results.

Summary and Conclusions

We propose an unsteady aerodynamic theory (i.e., a dynamic induced-flow theory) with the following advantages over conventional unsteady models:

1) *The model is based on first principles*. It is three-dimensional, unsteady acceleration-potential theory with arbitrary lift distribution and a finite number of blades. The rotor disc can be at any angle to the flow.

2) *The method is extremely flexible in application*. The user may choose the number of harmonics as well as the type and number of radial shape functions, including finite elements. Radial or harmonic coupling can be neglected if necessary, and

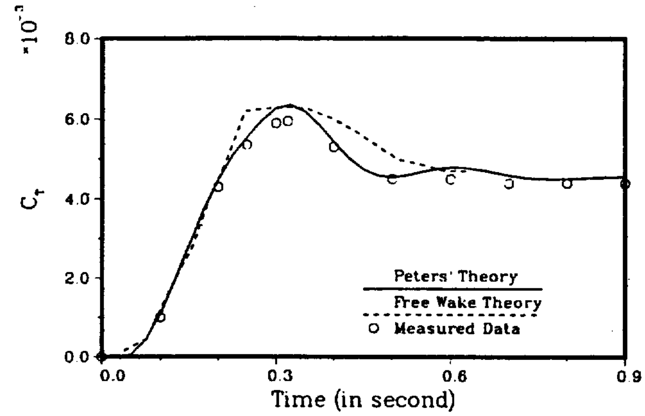

Fig. 9a. Time history of thrust due to ramp input for θ_0 of 12° at 48°/sec, σ = .042, p = 1.0, $B^4\gamma$ = 4.7, Q = 4.

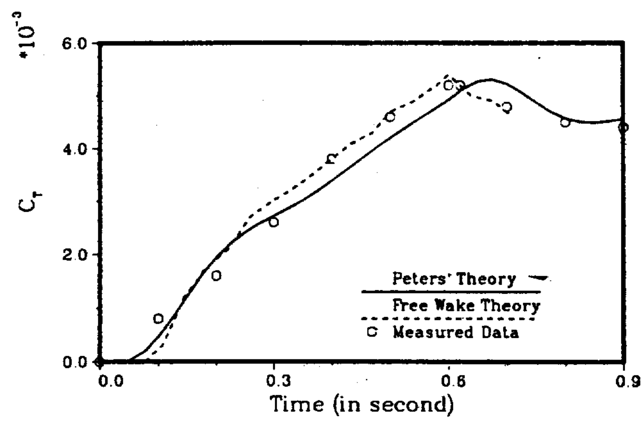

Fig. 9b. Time history of thrust due to ramp input for θ_0 of 12° at 20°/sec, σ = .042, p = 1.0, $B^4\gamma$ = 4.7, Q = 4.

the theory may be applied either as a perturbation theory or as a nonlinear theory.

3) *The method is easily used with other theories.* It may be applied either in the time or frequency domain and may be coupled to any blade-lift model (including dynamic-stall models, table look-up, compressible flow, and CFD computations in two-dimensions). All that is required is the augmentation of the user's equations with additional first-order state equations.

4) *The model is adaptable.* One may include simple correction factors to account for chordwise lift distribution, wake contraction, and ground effect.

5) *The theory recovers other theories.* Implicit in this model are Theodorsen theory, the Loewy and Miller functions, Prandtl/Goldstein theory, and dynamic inflow theory.

6) *The theory is not limited to flow at the blade.* Once the flow states are known at the rotor, the potential function provides pressures and velocities everywhere in the flow field.

7) *The theory shows good correlation with all data to which it has thus far been compared.* This includes collective and differential frequency response, response to transients in collective pitch, and laser flow measurements.

The limitations of the model are that it converges slowly and so does not easily capture flow discontinuities. It cannot provide detailed information close to the blade surface such as would be necessary for modeling blade-vortex interactions or acoustical phenomena. It is basically a prescribed-wake analysis and cannot account for wake roll-up. Thus, its usefulness is in the area of rotor aeroelasticity, Q/rev vibrations, and design of higher-harmonic controllers.

References

[1]Theodorsen, T., "General Theory of Aerodynamic Instabilities and the Mechanism of Flutter," NACA TR 496, 1949.

[2]Loewy, Robert G., "A Two-Dimensional Approach to the Unsteady Aerodynamics of Rotary Wings," *Journal of the Aerospace Sciences*, Vol. 24, (2), Feb 1957.

[3]Miller, R. H., "Rotor Blade Harmonic Air Loading," *AIAA Journal*, Vol. 2, (7), Jul 1964.

[4]Johnson, Wayne, *Helicopter Theory*, Princeton University Press, Princeton, N.J., 1980.

[5]Landgrebe, A. J., "The Wake Geometry of a Hovering Helicopter Rotor and Its Influence on Rotor Performance," *Journal of the American Helicopter Society*, Vol. 16, (4), Oct 1972.

[6]Rand, O. and Graber, A., "Free Wake Model of Hovering Rotors Having Straight or Curved Blades," International Conference on Rotorcraft Basic Research, Research Triangle Park, North Carolina, Feb 1985.

[7]Clark, D. R. and Leiper, A. C., "The Free Wake Analysis—a Method for the Prediction of Helicopter Rotor Hovering Performance," 25th Annual National Forum of the American Helicopter Society, Washington, D.C., May 1969.

[8]Kocurek, J. D. and Tangler, J. L., "A Prescribed Wake Lifting Surface Hover Performance Analysis," *Journal of the American Helicopter Society*, Vol. 22, (1), Jan 1977.

[9]Jones, J. P., "An Actuator-Disc Theory for the Shed Wake at Low Tip-Speed Ratios," MIT Aeroelasticity and Structures Laboratory, Technical Report 133-1, 1965.

[10]Ormiston, Robert A., "An Actuator-Disc Theory for Rotor Wake Induced Velocities," AGARD Specialists' Meeting on the Aerodynamics of Rotary Wings, Marseille, France, Sep 1972, AGARD CP-III.

[11]Baskin, V. Ye, et al., "Theory of Lifting Airscrews," NASA TTF-823, 1975.

[12]Wang, Shi-cun and Xu, Zhi, "A Simplified Method for Predicting Rotor Blade Airloads," Seventh European Rotorcraft and Powered Lift Aircraft Forum, Garmisch, W. Germany, Sep 1981.

[13]Gangwani, S., "Prediction of Dynamic Stall and Unsteady Airloads for Rotor Blades," Proceedings of the 37th Annual Forum of the American Helicopter Society, New Orleans, Louis., May 1981.

[14]Tran, C. T. and Petot, D., "Semi-Empirical Model for the Dynamic Stall of Airfoil in View of the Application to the Calculation of Responses of a Helicopter Blade in Forward Flight," *Vertica*, Vol. 6, 1982.

[15]Wake, Brian E. and Sankar, Lakshi N., "Solutions of the Navier Stokes Equations for the Flow about a Rotor Blade," Proceedings of the National Specialists' Meeting on Aerodynamics and Aeroacoustics, Arlington, Tex., Feb 1987.

[16]Bisplinghoff, Ashley, and Halfman, *Aeroelasticity*, Addison-Wesley, Reading, Mass., 1955.

[17]Dinyavari, M. A. H. and Friedmann, P. P., "Unsteady Aerodynamics in Time and Frequency Domains for Arbitrary Motion of Rotary Wings in Hover and Forward Flight," AIAA SDM Conference, Palm Springs, Calif., May 1984, AIAA-84-0988.

[18]Friedmann, P. P. and Venkatesan, C., "Finite State Modeling of Unsteady Aerodynamics and Its Application to a Rotor Dynamics Problem," Eleventh European Rotorcraft Forum, London, Sep 1985, paper No. 72.

[19]Elliott, Andrew S., "Rotor-Body Response to Atmospheric Turbulence Using a Two-Dimensional Unsteady Aerodynamic Model," Presented at the Robert F. Lichten Competition, Southeast Region of the American Helicopter Society, NASA Langley Research Center, Feb 10, 1987.

[20]Kinner W., "Theory of the Circular Wing," Ingenieur Archiv, Vol. 7, 1937, Translation No. 2345, Ministry of Aircraft Production, U.K.

[21]Mangler, K. W. and Squire, H. B., "The Induced Velocity Field of a Rotor," Reports and Memoranda No. 2642, 1950.

[22]Joglekar, M. and Loewy, R., "An Actuator-Disc Analysis of Helicopter Wake Geometry and the Corresponding Blade Response," USAAU-LABS Technical Report 69-66, 1970.

[23]Pitt, Dale M. and Peters, David A., "Theoretical Prediction of Dynamic Inflow Derivatives," *Vertica*, Vol. 5, 1981.

[24]Gaonkar, Gopal H., et al., "The Use of Actuator-Disc Dynamic Inflow for Helicopter Flap-Lag Stability," *Journal of the American Helicopter Society*, Vol 28, (3), Jul 1983.

[25]Schade, Th. and Krienes, K., "The Oscillating Circular Airfoil on the Basis of Potential Theory," Luftfahrtforschung, Vol. 17, No. 11-12, Dec. 10, 1940, and Vol. 19, No. 8, Aug. 20, 1942, NACA TM No. 1098, Feb 1947.

[26]Gradshteyn, I. S. and Ryzhik, I. M., *Table of Integrals, Series, and Products*, Corrected and Enlarged Edition, Academic Press, New York, 1980.

[27]Abramowitz, Milton and Stegun, Irene A., *Handbook of Mathematical Functions*, Ninth Edition, Dover, New York, 1972.

[28]Peters, David A. and He, Cheng Jian, "A Closed-Form Unsteady Aerodynamic Theory for Lifting Rotors in Hover and Forward Flight," Proceedings of the 43rd Annual Forum of the American Helicopter Society, St. Louis, Mo., May 18–20, 1987.

[29]Johnson, Wayne, *Helicopter Theory*, Princeton University Press, Princeton, N.J., 1980.

[30]Peters, David A. and HaQuang, Ninh, "Dynamic Inflow for Practical Applications," *Journal of the American Helicopter Society*, Vol. 33 (4), Oct 1988.

[31]Ham, Moser, and Zvara, "Investigation of Rotor Response to Vibratory Aerodynamic Inputs: Part I. Experimental Results and Correlation with Theory," WADC Technical Report 58-87, Wright Air Development Center, Oct 1958.

[32]Berry, John D., Hoad, Danny R., Elliott, Joe W., and Althoff, Susan L., "Helicopter Rotor Induced Velocities: Theory and Experiment," Proceedings of the National Specialists' Meeting on Aerodynamics and Aeroacoustics, Arlington, Tex., Feb 1987.

[33]Quackenbush, Todd R., "Computational Studies in Low Speed Rotor Aerodynamics," Proceedings of the National Specialists' Meeting on Aerodynamics and Aeroacoustics, Arlington, Tex., Feb 1987.

[34]Johnson, Wayne, *Helicopter Theory*, Princeton University Press, Princeton, N.J., 1980.

[35]Peters, David A., and He, Cheng Jian, "Comparison of Measured Induced Velocities with Results from a Closed-Form Finite State Wake Model in Forward Flight," presented at the 45th Annual Forum of the American Helicopter Society, Boston, Mass., May 22–24, 1989.

[36]Carpenter, P. J. and Fridovich, B., "Effect of Rapid Blade Pitch Increase on the Thrust and Induced Velocity Response of a Full Scale Helicopter Rotor," NACA TN 3044, Nov 1953.

[37]Crews, S. T., Hohenemser, K. H., and Ormiston, R. A., "An Unsteady Wake Model for a Hingeless Rotor," *Journal of Aircraft*, Vol. 11, (1), Jan 1974.